Accepted Manuscript

Fluorescent turn-on sensors based on pyrene-containing Schiff base derivatives for Cu^{2+} recognition: spectroscopic and DFT computational studies

Zannatul Kowser, Cheng-Cheng Jin, Xuekai Jiang, Shofiur Rahman, Paris E. Georghiou, Xin-Long Ni, Xi Zeng, Carl Redshaw, Takehiko Yamato

PII: S0040-4020(16)30530-0

DOI: 10.1016/j.tet.2016.06.017

Reference: TET 27831

To appear in: *Tetrahedron*

Received Date: 25 May 2016

Accepted Date: 6 June 2016

Please cite this article as: Kowser Z, Jin C-C, Jiang X, Rahman S, Georghiou PE, Ni X-L, Zeng X, Redshaw C, Yamato T, Fluorescent turn-on sensors based on pyrene-containing Schiff base derivatives for Cu^{2+} recognition: spectroscopic and DFT computational studies, *Tetrahedron* (2016), doi: 10.1016/j.tet.2016.06.017.

Graphical Abstract

To create your abstract, type over the instructions in the template box below.
Fonts or abstract dimensions should not be changed or altered.

Fluorescent turn-on sensors based on pyrene-containing Schiff base derivatives for Cu^{2+} recognition: Spectroscopic and DFT computational studies

Leave this area blank for abstract info.

Zannatul Kowser,[a] Cheng-Cheng Jin,[a] Xuekai Jiang,[a] Shofiur Rahman,[b] Paris E. Georghiou,[b] Xin-Long Ni,[c] Xi Zeng,[c] Carl Redshaw[d] and Takehiko Yamato*[a]

[a] *Department of Applied Chemistry, Faculty of Science and Engineering, Saga University, Honjo-machi 1, Saga 840-8502, Japan*

[b] *Department of Chemistry, Memorial University of Newfoundland, St. John's, Newfoundland and Labrador, Canada A1B3X7*

[c] *Key Laboratory of Macrocyclic and Supramolecular Chemistry of Guizhou Province, Guizhou University, Guiyang 550025, People's Republic of China*

[d] *Department of Chemistry, The University of Hull, Cottingham Road, Hull, Yorkshire, HU6 7RX, UK*

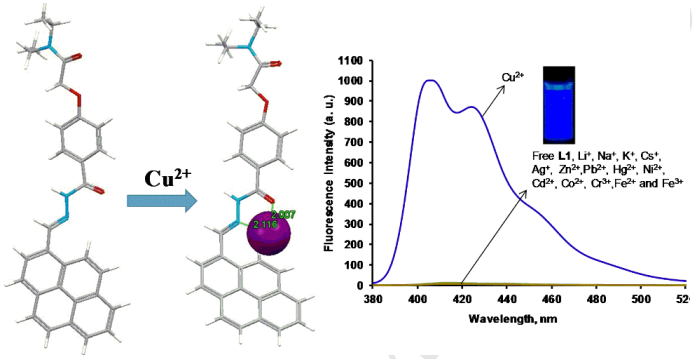

Tetrahedron
journal homepage: www.elsevier.com

Fluorescent turn-on sensors based on pyrene-containing Schiff base derivatives for Cu^{2+} recognition: Spectroscopic and DFT computational studies

Zannatul Kowser,[a] Cheng-Cheng Jin,[a] Xuekai Jiang,[a] Shofiur Rahman,[b] Paris E. Georghiou,[b] Xin-Long Ni,[c] Xi Zeng,[c] Carl Redshaw[d] and Takehiko Yamato*[a]

[a] *Department of Applied Chemistry, Faculty of Science and Engineering, Saga University, Honjo-machi 1, Saga 840-8502, Japan*
[b] *Department of Chemistry, Memorial University of Newfoundland, St. John's, Newfoundland and Labrador, Canada A1B3X7*
[c] *Key Laboratory of Macrocyclic and Supramolecular Chemistry of Guizhou Province, Guizhou University,Guiyang 550025, People's Republic of China*
[d] *Department of Chemistry, The University of Hull, Cottingham Road, Hull, Yorkshire, HU6 7RX, UK*

ARTICLE INFO

Article history:
Received
Received in revised form
Accepted
Available online

Keywords:
Pyrene-based Schiff base derivatives
Fluorescent turn-on sensor
High selectivity and sensitivity
DFT computational studies

ABSTRACT

A new fluorescent chemosensor **L1**, pyrene containing long chain Schiff base derivative in 1-position has been synthesized. Similarly, the receptors **L2** and **L3** are also designed in order to compare the binding ability for detection of Cu^{2+}. The receptors exhibit very weak fluorescence (Φ = 0.01) due to the photoinduced electron transfer (PET). Upon addition of 10 equiv. of Cu^{2+}, the emission intensity of ligands **L1** and **L2** are increased 65-fold (Φ = 0.31) and 25-fold (Φ = 0.08) in CH_3CN/CH_2Cl_2 solvents system respectively. NMR titration experiments, spectroscopic and DFT computational studies confirmed binding phenomena and sensitivity of Cu^{2+}.

1. Introduction

The development of selective and sensitive chemosensors for the recognition of cations and anions of biological interest has been a subject of current research in recent years given that they play an important role in many environmental and biological processes.[1–4] Amongst the various essential metal ions in the human body, copper is the third most abundant transition metal ion. Copper as a catalytic cofactor, plays a crucial role for a variety of metal enzymes including superoxide dismutase, cytochrome oxidase and tyrosinase. However, if excessive amounts are ingested, exposure to a high level of copper may result in neurodegenerative diseases as it is involved in the production of reactive oxygen species.[5] Furthermore, in addition, high levels of ingested copper causes gastrointestinal disturbance even when present for a short period of time, whilst over longer periods, liver or kidney damage may also occur.[6] Thus although copper is essential for life, it can also be highly toxic to organisms. For these reasons, Cu^{2+} is one of the most frequently studied metal ions of the first row transition metals in the area of chemosensors.[7, 8] Beside this, Cu^{2+} has the highest formation constant with ligands which contain oxygen or nitrogen donor atoms.[9] Therefore, the development of highly selective chemosensors for the copper ion in the presence of various metal ions is attracting growing interest. Of the sensors reported to-date, several advantages for fluorescent chemosensors over other methods have been noted. These include their sensitivity, specificity and real time monitoring with a fast response time.[10] Although fluorescent chemosensors for the copper ion have been widely investigated,[11] there are still only some examples of "off-on" sensors.[12] As Cu^{2+} is a fluorescence quencher, owing to its paramagnetic nature,[13] most fluorescent sensors bind Cu^{2+} by the fluorescence quenching process which involves a charge-, or energy-transfer mechanism.[14] Fluorescence quenching is unfavourable for a high signal output and also hampers the temporal separation of spectroscopically similar complexes with time-resolved fluorometry.[15] Considering this factor, Yoon et al. have synthesized a highly selective and ratiometric 'off-on' sensor, namely a rhodamine-pyrene derivative for Cu^{2+} detection.[16]

Many fluorescence mechanisms have also been reported based on photoinduced electron transfer (PET), intermolecular charge transfer (ICT), excited state intramolecular proton transfer (ESIPT), excimer formation and non-coordinative interations between a ligand and the metal ion. In the case of PET, there is little or no change of the spectral shifts with changes of emission intensities, whereas both spectral shifts and intensity changes are observed for ICT, ESIPT also shows fluorescence enrichment with or without accompanying spectral changes. Furthermore, excimer emission typically provides a broad fluorescence band without vibrational structure, with the maximum shifted, in the case of most aromatic molecules.[17] In order

* Corresponding author. Fax: +81 952 28 8548; e-mail address: yamatot@cc.saga-u.ac.jp (T. Yamato).

to develop the fluorescence intensity enhancement of the receptor upon binding of Cu^{2+} via a photoinduced intramolecular electron transfer, one needs to carefully choose or design the receptor molecule containing a fluorophore. The fluorescence quenching needs to be maximized in the free receptor responsible for the PET, whereas the PET should be minimized in the Cu^{2+}-bound state of the receptor. Among different fluorophore units, pyrene is the most useful due to its high fluorescence quantum yield, chemical stability, and long fluorescence lifetime. Additionally, pyrene exhibits monomer-excimer dual fluorescence, and the fluorescence intensity ratio of the monomer-to-excimer emission is sensitive to conformational changes of the pyrene-functionalized system.[11a,18] Consequently, several pyrene-based sensors have been constructed for metal ion detection.[19] Based on monomer-excimer conversion, a pyrene chemosensor containing a thiophene moiety was a highly selective and ratiometric fluorescent sensor which induces the dual appearance of excimer emission and disappearance of monomer emission after addition of Cu^{2+} ion.[20] Venkatesan and Wu. have designed a pyrene-based fluorescent probe bearing the hydrazinyl pyridine moiety for Cu^{2+} ion detection based on the PET mechanism. The chemosensors binding with the metal ion block the PET mechanism resulting in significant fluorescence enhancement.[21] Furthermore, Wu et al. have developed a highly selective turn-on fluorescence sensor for Cu^{2+} detection in living cells, in which the picolinohydrazide act as a chelator and can bind to Cu^{2+} through two functional groups, namely the amide nitrogen atom and the pyridine nitrogen atom.[22]

On the basis of the above, we have focused our interest on designing molecules which can serve as receptors to recognize cations based on a fluorescence 'off-on' mechanism. In this regard, we have utilized Schiff base derivatives in which a hydrazido carbonyl group binds with the pyrene moiety, whilst a diethylaminocarbonylmethoxy group forms the upper part of the phenyl ring for the formation of the receptor ligand **L1** (Scheme 1). Receptors **L2** and **L3** were also synthesized: a methoxy instead of the diethylaminocarbonylmethoxy group was present in **L2** whilst only a phenylimino moiety instead of a hydrazido carbonyl group was present in **L3**. Ligands **L1** and **L2** can bind and sense Cu^{2+} by fluorescence through the coordination bond with the hydrazidocarbonyl group, following a 1:1 ligand to metal binding mode. Interestingly, in case of ligand **L1,** the upper part, *N*,*N*-diethylaminocarbonylmethoxy group has prominent effect upon binding with Cu^{2+}.

The probes show very weak fluorescence (Φ = 0.01) at 405 nm due to PET. When binding with Cu^{2+}, ligand **L1** induces a blue emission (intensity Φ = 0.31) by inhibiting the PET, and the emission intensity is approximately 65 times greater than that of the free ligand. Furthermore, in comparison with the receptors **L2** and **L3**, ligand **L1** is highly sensitive for Cu^{2+} detection due to the strong inhibition of PET and the different binding phenomenon of ligand to metal complex.

2. Results and discussions

2.1. Synthesis

The synthetic pathways of the fluorogenic molecules **L1**, **L2** and **L3** are similar, and are summarized in Scheme 1. The amidation of compound **1** was carried out with hydrazine in a solution mixture of EtOH to synthesize 4-(hydrazidocarbonyl)(*N*,*N*-diethylaminocarbonylmethoxy)benzene **2**. Compound **2** was then condensed with 1-pyrenecarbaldehyde to give **L1**. Following a similar reaction pathway, the reference compound **L2** was prepared from ethyl-*p*-anisate in order to compare the binding affinities for Cu^{2+}. Ligand **L3** was also synthesized from the condensation reaction of Py-CHO with 4-methoxyanisidine. Reference compounds **L2**[23] and **L3**[24] were prepared following the reported procedures. The structures of compounds **L1**, **L2** and **L3** were characterized by ^{1}H and ^{13}C NMR spectroscopy and are given in the ESI (Figures. SI 16–SI 20). IR spectra, FAB-MS and elemental analysis were taken to confirm the structure of ligand **L1**.

2.2. Binding studies

At first, the cation-binding properties of compounds **L1**, **L2** and **L3**, featuring the Schiff-base sites and armed with the pyrene moiety, were characterized by spectroscopic measurements. These were carried out in CH_3CN/CH_2Cl_2 (1000:1, v/v) by addition of different metal cations Li^+, Na^+, K^+, Cs^+, Ag^+, Zn^{2+}, Cu^{2+}, Pb^{2+}, Hg^{2+}, Fe^{2+} and Fe^{3+} (perchlorate salts), Ni^{2+}, Cd^{2+}, Co^{2+}, Cr^{3+} (nitrate salts) dissolved in CH_3CN. As shown in Fig. 1, the UV−vis absorption

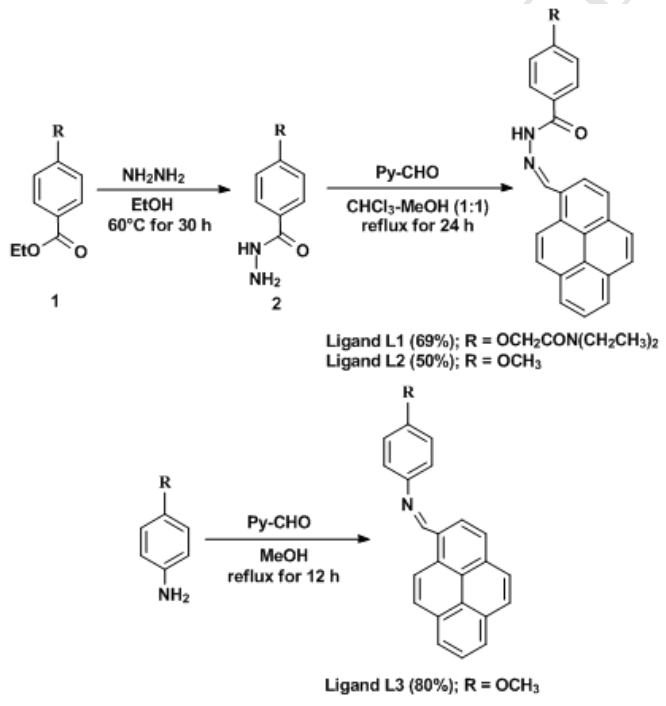

Scheme 1 Synthesis of receptors **L1, L2** and **L3.**

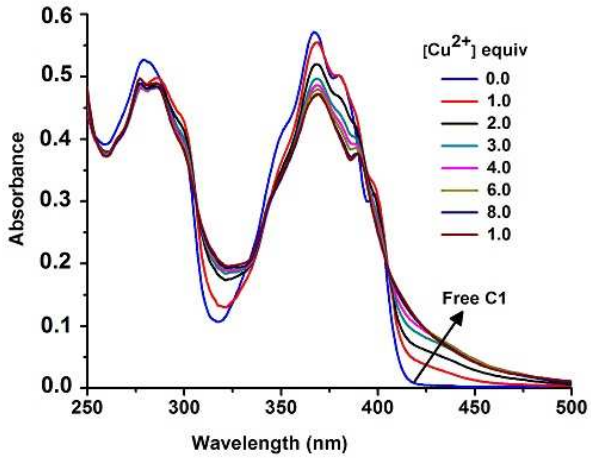

Fig. 1 UV-vis spectra of ligand **L1** (10.0 μM) in CH_3CN/CH_2Cl_2 (1000:1, v/v) upon addition of 10 equiv. of Cu^{2+} metal ions as their aqueous solution.

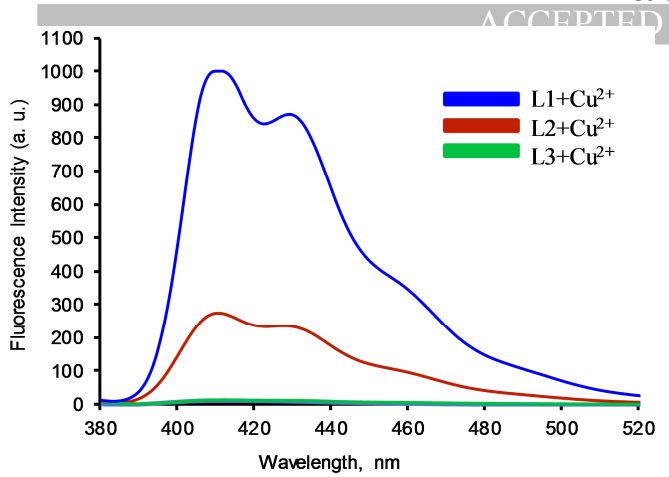

Fig. 2 Fluorescence response of ligands **L1**, **L2** and **L3** (1.0 μM) upon addition of Cu^{2+} ions (10 equiv.) measured in CH_3CN/CH_2Cl_2 (1000:1, v/v). λ_{ex} = 367 nm.

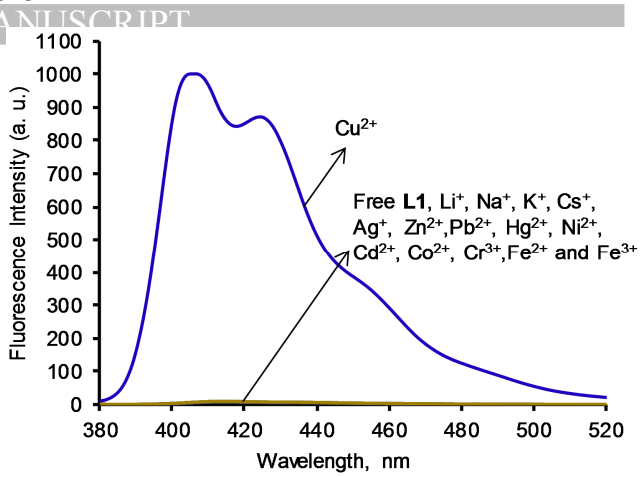

Fig. 3 Fluorescence spectra of ligand **L1** (1.0 μM, λ_{ex} = 367 nm) upon addition of various metal ions (10 equiv.) as their CH_3CN solutions.

spectra of ligand **L1** exhibited typical pyrene absorption bands at 277 and 349 nm along with a LE broad band centered at 367 nm, attributed to the hydrazido carbonyl group as well as the diethylaminocarbonylmethoxy group of the upper part. Upon addition of up to 10 equiv. of Cu^{2+} to the solution of ligand **L1**, the absorbance at 367 nm decreased progressively and at the same time, a new UV−vis absorption band at around 430 nm was observed; two identical isosbestic points were observed at around 305 and 410 nm indicating the presence of a unique complex after addition of Cu^{2+}. The resulting titration data suggests strong interactions between ligand **L1** and Cu^{2+}.

Ligands **L1, L2** and **L3** (1.0 μM, λ_{ex} = 367 nm) showed only very weak fluorescence in CH_3CN/CH_2Cl_2 (1000:1, v/v). The emission intensity of the pyrenyl fluorophore is quenched because the lone pair electrons from the nitrogen atoms are transferred to the excited pyrenyl moiety. After the addition of small concentrations of Cu^{2+}, preferential binding occurs to terminate the PET. Before and after addition of Cu^{2+}, the fluorescence intensity changes of ligand **L1** are compared with **L2** and **L3** and it can be seen that the free ligand **L1** exhibits higher fluorescence intensity than **L2** and **L3** (Figure SI 8). Fig. 2 shows that after addition of Cu^{2+}, the fluorescence intensity is predominantly enhanced. In the case of **L1**, which is enhanced approximately 40 times more than **L2** and 57 times more than **L3.** This suggests that PET occurs predominantly in **L3** versus **L2** and then **L1**. To elucidate the binding properties of **L1** towards other metal ions, the fluorescence changes upon addition of a wide range of metal cations (10 equiv.) using their perchlorate salts and nitrate salts in CH_3CN solution were determined. As shown in Fig. 3, ligand **L1** exhibited high selectivity toward Cu^{2+} ions. By contrast, the addition of different metal cations Li^+, Na^+, K^+, Cs^+, Ag^+, Zn^{2+}, Cu^{2+}, Pb^{2+}, Hg^{2+}, Fe^{2+}, Fe^{3+}, Ni^{2+}, Cd^{2+}, Co^{2+} and Cr^{3+} resulted in almost no fluorescence enhancement.

The binding property of probe **L1** with Cu^{2+} (Fig. 4) was then determined by a fluorescence titration experiment. When excited at 367 nm, **L1** displayed a weak emission band at about 405 nm. The stepwise addition of Cu^{2+} leads to an increase of fluorescence intensity. The fluorescence intensity is increased by 65-fold upon the addition of 10 equiv. of Cu^{2+} in CH_3CN/CH_2Cl_2 (1000:1, v/v) The resulting binding or association constant determined by a global analysis[25a], for the **L1**-Cu^{2+} complexation, was $1.29 \times 10^5 \pm 0.32\%$ M^{-1} value. The covariance of fit value was < 0.01 which is a reasonably good fit of the data to the 1:1 binding model (Figure SI 9). The Benesi-Hildebrand plot gave a smaller value of 6.12×10^4 M^{-1} and the limitations of the B-H method has been well-addressed in the literature.[25a,b] The global analysis approach offers a more accurate determination of the equilibria involved since it avoids the manipulation of the actual experimental data to effect linear relationship was observed between the fluorescence intensity and the concentration of Cu^{2+} showing a low detection limit of 8.80×10^{-8} M.[26a] This value is much lower than the concentration allowed in drinking water according to the US EPA (20 μM).[20] Furthermore, when excited at 367 nm, the quantum yield, Φ, of the **L1**-Cu^{2+} complex was 0.31 which was 31-fold more enhanced than of free ligand **L1** alone.[26b] The fluorescence titration experiments of Cu^{2+} complex was 0.31 which was 31-fold more enhanced than of free ligand **L1** alone.[26b] The fluorescence titration experiments of Cu^{2+} with **L2** were also conducted in the same CH_3CN/CH_2Cl_2 solvent mixture and revealed an 8-fold enhancement in the quantum yield over the free ligand **L2** (Figure SI 6). The global fit analysis[25a] (Figure SI 10) for the binding or association constant of **L2** was determined to be $1.55 \times 10^4 \pm 0.24\%$ M^{-1} (cov fit < 0.01) and was found to have a detection limit of 4.94×10^{-7} M (Figure SI 12). In this case, the quantum yield is enhanced only 8-fold after addition of Cu^{2+} (Φ = 0.08). On the other hand, the minor changes in the fluorescence titration spectra of **L3** indicate the very weak coordination with Cu^{2+} (Figure SI 7). There are also insignificant changes of the photophysical properties of ligand **L3**. These results confirm that ligand **L1** is more sensitive and exhibits a stronger affinity toward Cu^{2+} than **L2** and **L3** in CH_3CN/CH_2Cl_2 (Table 1).

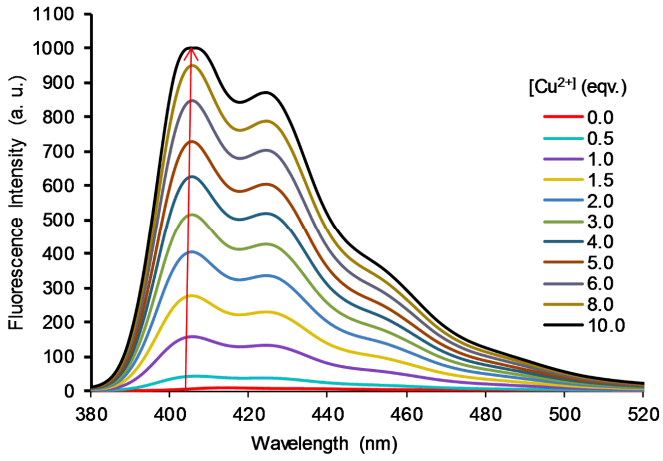

Fig. 4 Fluorescence spectra of ligand **L1** (1.0 μM) upon addition of increasing concentration of Cu^{2+} ions (0–10 equiv.) measured in CH_3CN/CH_2Cl_2 (1000:1, v/v). λ_{ex} = 367 nm.

Table 1. Photophysical properties of ligands **L1**, **L2** and **L3** with their Cu^{2+} complexes.

Comp.	K_a (M^{-1})[a]	LODs (M)[b]	Φ[c]	(Φ) enhanced[d]
L1⊃Cu^{2+}	1.29×10^5	8.80×10^{-8}	0.31	31-fold
L2⊃Cu^{2+}	1.55×10^4	4.94×10^{-7}	0.08	8-fold
L3⊃Cu^{2+}	NA	NA	0.01	NA

[a]K_a = Association constant; [b]LODs = Detection limits (measured from fluorescence titration experiments); [c]Φ = Quantum yield of **L1**⊃Cu^{2+}; [d](Φ) enhanced = Difference between the quantum yield of free ligand and after addition of Cu^{2+}; NA means fluorescence change was scarcely observed; photophysical properties cannot be calculated.

Moreover, the association constant of the pyrene containing the picolinohydrazide moiety was found to be 2.75×10^3 M^{-1}.[22] On the basis of the findings above, it is suggested that ligand **L1** is a highly sensitive fluorescent probe than **L2** and **L3** in CH_3CN/CH_2Cl_2 (1000:1, v/v). The coordination of Cu^{2+} with the Schiff base site presumably caused the inhibition of PET effect which was much stronger than any cavity-control effect. Furthermore, upon addition of metal ions (10.0 μM) to the receptor **L1** (1.0 μM) and Cu^{2+} (10.0 μM), all of the competitive cations caused no significant interference at higher concentration. These results indicate that **L1** displays an excellent selectivity toward Cu^{2+} over the other metal cations (Fig. 5). In order to quantify the stoichiometry of the complexes **L1**-Cu^{2+}, a Job's plot analysis was carried out in which the emission of the complexes at 405 nm were plotted against molar fractions of **L1** and Cu^{2+} under the conditions of an invariant total concentration. The fluorescence intensity shows a maximum at the mole fraction 0.5 which corresponds to a 1:1 ratio of **L1**⊃Cu^{2+} complex (Figure SI 13).

A ^{1}H NMR spectroscopic analysis with **L1** was performed to investigate the nature of the co-ordination structure of **L1** and Cu^{2+}. Since the receptor **L1** was only partially soluble in $CD_3CN/CDCl_3$, a 9:3 ratio of $CDCl_3$/DMSO-d_6 was employed for these analyses. Copper ion has paramagnetic nature, therefore when binding occurs, the proton signals close to the binding site is easily affected by Cu^{2+}.[22] Fig. 7 shows that, upon addition of Cu^{2+}, the proton (amide NH_a) signal at δ 11.7 ppm completely disappeared. This result indicates the influence of Cu^{2+} on the amide NH group. In addition, the proton H_b (CH=N) also disappeared at about δ = 9.55 ppm. Furthermore, Cu^{2+} addition leads to a large downfield shift of 0.5 and 0.54 ppm for the pyrene proton H_c, and the phenyl ring proton H_d, respectively (Table 2). The other phenyl ring protons also shifted from δ = 8.12 ppm to δ = 8.30 ppm. These protons are broad and have lower intensities. The phenyl proton shifts are due to the inductive effect of the diethylaminocarbonylmethoxy group which overlapped with other pyrene protons. Moreover, the methylene proton H_e and ethyl protons H_g and H_f also underwent slight upfield shifts of 0.05 and 0.06 and 0.04 ppm, respectively. In contrast, in order to clarify the co-ordination structure of ligand **L1**, ^{1}H NMR analysis of ligand **L2** was also performed in presence of Cu^{2+} ion (Figure SI 14). In this case, like with ligand **L1**, the amide proton, H_a and imine proton H_b of **L2** disappeared due to the paramagnetic nature of Cu^{2+}. On the other hand, the pyrene proton H_c and the phenyl ring proton H_d induced smaller downfield shift of 0.16 and 0.26 ppm than with ligand **L1**⊃Cu^{2+}. The other phenyl ring protons overlapped with the pyrene protons and the chemical shifts remain unchanged. In addition to this, there is no change in the methoxy proton H_e which signifies that the methoxy protons have no contribution to the binding. These results indicate that Cu^{2+} ions are only bound to the imine nitrogen atom and the amide carbonyl oxygen of ligand **L2**. Also, up to the addition of 1 equiv. of Cu^{2+}, the prominent changes which were monitored represent 1:1 complexes. Furthermore, to gain a further understanding of the binding stoichiometry of **L1** and Cu^{2+} complex, ^{13}C NMR titration experiments were carried out in a mixture of $CDCl_3$/DMSO

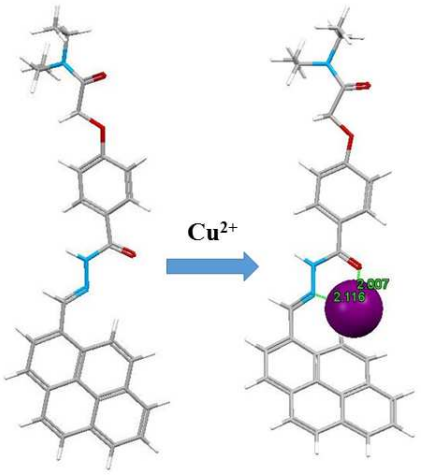

Fig. 6 Geometry-optimized (PBE0/LANL2DZ) structures of **L1** with complex Cu^{2+} ion, *Left*: The free ligand **L1** (Ellipsoid); *Right:* Ligand **L1** complex with Cu^{2+} ion (Ellipsoid). Colour code: carbon = dark grey and oxygen atom = red, nitrogen = blue and Cu^{2+} = purple.

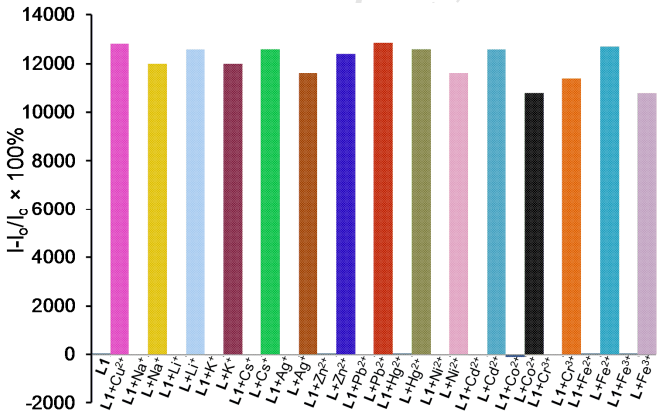

Fig. 5 Fluorescence response of **L1** (1.0 μM) in CH_3CN/CH_2Cl_2 (1000:1, v/v) to 10.0 μM of various tested metal ions and to the mixture of 10.0 μM of tested metal ions with 10.0 μM Cu^{2+} ion. Here **L** represents the emission intensity of ligand **L1** in the presence of Cu^{2+}. I_0 is the fluorescence intensity of free **L1**, and *I* is the fluorescence intensity after addition of metal ions at 405 nm.

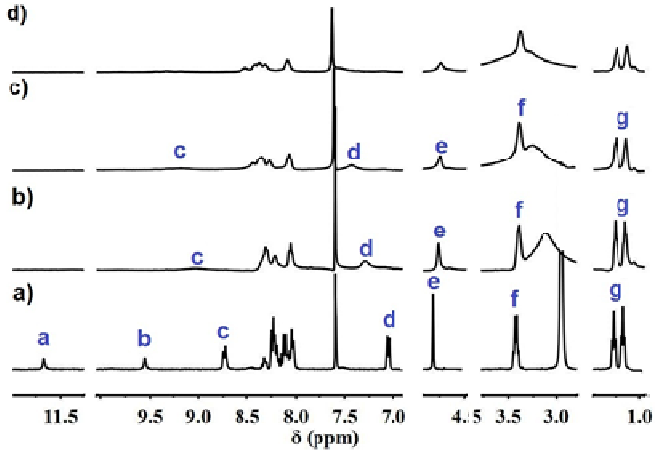

Fig. 7 Partial ^{1}H-NMR titration of **L1**/guest (H/G = 1:1); (a) Free ligand **L1** (8.60×10^{-3} M); (b) **L1**⊃Cu^{2+} (0.5 equiv.) (c) **L1**⊃Cu^{2+} (1 equiv.); (d) **L1**⊃Cu^{2+} (2 equiv.). Solvent: $CDCl_3$–DMSO (9:3, v/v). 400 MHz at 298 K.

Table 2. ^{1}H NMR chemical shift differences of free **L1** and **L2** with **L1**⊃Cu^{2+} and **L2**⊃Cu^{2+}, respectively.[a]

	δ_{ppm} in **L1** (H/G = 1:1)			δ_{ppm} in **L2** (H/G = 1:1)		
	Free **L1**	**L1**⊃Cu^{2+}	Δδ	Free **L2**	**L2**⊃Cu^{2+}	Δδ
H_a	11.66	----	----	11.79	----	----
H_b	9.55	----	----	9.58	----	----
H_c	7.06	7.56	0.50	7.04	7.21	0.16
H_d	8.74	9.28	0.54	8.77	8.96	0.26
H_e	4.81	4.75	0.05	3.92	3.91	0.01

[a] Δδ Values are the difference of the chemical shift between free ligand **L1** or **L2** and complexation with Cu^{2+}.

(Figure SI 15). The diethylaminocarbonylmethoxy, carbonyl carbon C1, and the hydrazido carbonyl carbon C2, of **L1** were first identified by comparison with **L2**. Upon the addition of Cu^{2+}, the C2 and C3 peaks of the ligand **L1** disappeared completely and the resonances corresponding to the C1 carbon mostly disappeared. ^{1}H NMR analysis revealed that the changes are almost terminated after addition of 1.0 molar equiv. of Cu^{2+} which is indicative of a 1:1 binding complex formation. It is also proposed that ligand **L1** forms a complex with Cu^{2+} by strong coordination with the hydrazidocarbonyl moiety. In this case, Cu^{2+} is coordinated with the imine nitrogen atom and amide carbonyl oxygen of ligand **L1**. Furthermore, the diethylaminocarbonylmethoxy group also has a prominent influence through an inductive effect on the **L1**⊃Cu^{2+} complexation.

A DFT computational study was also undertaken to shed further light on the binding mode of the ligand with Cu^{2+}. The geometries of the molecular structures were optimized with the PBE0 functional with the LANL2DZ basis set. The DFT level of theory using the hybrid Perdew-Burke-Ernzerhof parameter free-exchange correlation functional PBE0 (PBE1PBE in the Gaussian realization)[27] with the Hay and Wadt effective core potential LANL2DZ basis set was employed.[28] The starting structure was first generated using *SpartanPro10* with the MMFF94 method.[29] The generated structures were then imported into *Gaussian-09 Revision D.01*[30] and were geometry-optimized in the gas-phase. The calculated interactionenergy (IE) for each of **L1**⊃Cu^{2+} and **L2**⊃Cu^{2+} are -1519.2 and -1467.8 kJ mole^{-1}, respectively (See SI section for details). The DFT binding mode of the guest Cu^{2+} ion involves strong coordination with the hydrazidocarbonyl moiety of the ligands **L1** and **L2**. Furthermore, from the computed IE data, **L1**⊃Cu^{2+} is energetically favoured by 50.2 kJ mole^{-1} over the corresponding **L2**⊃Cu^{2+} complex, which is in agreement with the trend for the observed complexation data obtained by fluorescence titration experiments. This finding is also in agreement with the observed changes in the chemical shifts of the surrounding hydrazidocarbonyl moiety of both ligands and the changes of the chemical shifts of the upper part of ligand **L1.** The interaction energy (IE) for each complex was calculated according to equation (1):

$$\mathbf{IE} = \mathbf{E_{Complex}} - \mathbf{\Sigma(E_{ligand} + E_{Cu^{2+}}\ ion)} \qquad \mathbf{(1)}$$

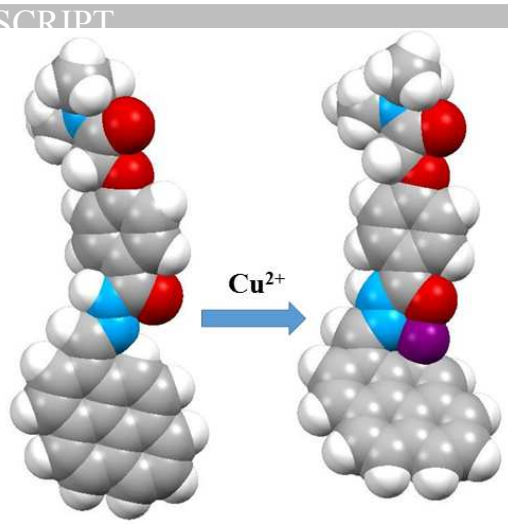

Fig. 8 Geometry-optimized (PBE0/LANL2DZ) structures (Space fill) of **L1** and as its Cu^{2+} complex ion. *Left*: The free ligand **L1**; *Right:* 1:1 **L1**⊃Cu^{2+} complex. Colour code: carbon = drack grey and oxygen atom = red, nitrogen = blue and Cu^{2+} = purple.

3. Conclusion

In conclusion, fluorogenic molecules **L1**, **L2** and **L3** which are pyrene-based Schiff base derivatives have been designed in order to compare their binding affinities for Cu^{2+} detection where the probes worked as a fluorescence "turn off-on" sensor. A PET mechanism was exploited to afford a convenient analytical strategy. The sensing ability and photophysical properties are well-supported by the fluorescence spectra and NMR titration experiments. The hydrazidocarbonyl moiety **L1** and **L2,** are strongly co-ordinated with Cu^{2+}. Moreover, the upper part of **L1** has a noticeable effect upon the binding of the complex of **L1**⊃Cu^{2+} which is also supported by DFT computational studies. Consequently, receptor **L1** acquires a higher affinity (65-fold enhanced) in comparison with compound **L2** (25-fold) and **L3** exhibits very weak fluorescence enhancements (7-fold) for Cu^{2+} detection.

4. Experimental

4.1. General

^{1}H and ^{13}C NMR spectra were recorded on a Nippon Denshi JEOL FT-300 NMR spectrometer and Varian-400MR-vnmrs400 with SiMe4 as an internal reference: J-values are given in Hz. IR spectra were measured for samples as KBr pellets in a Shimadzu FTIR-8400 spectrophotometer. Mass spectra were obtained with a Nippon Denshi JMS-HX110A Ultrahigh Performance Mass Spectrometer at 75 eV using a direct-inlet system. Elemental analyses were performed by a Yanaco MT-5. UV-vis spectra were recorded using a Shimadzu UV-3150UV-vis-NIR spectrophotometer. Fluorescence spectroscopic studies of compounds in solution were performed in a semimicro fluorescence cell (Hellma®, 104F-QS, 10 × 4 mm, 1400 μL) with a Varian Cary Eclipse spectrophotometer. Fluorescence quantum yields were recorded in solution (Hamamatsu Photonics K. K. Quantaurus-QY A10094) using the integrated sphere absolute PL quantum yield measurement method. Unless otherwise stated, all reagents used were purchased from commercial sources and were used without further purification. All the solvents used were dried and distilled by the usual procedures before use. All melting points (Yanagimoto MP-S1) are uncorrected.

4.2. Materials

*4.2.1. Synthesis of Compound **2**.* To **1** (300 mg, 1.19 mmol) in a round-bottom flask, ethanol (18 mL) and hydrazine hydrate (3.0 mL) were added and with stirring, the temperature was maintained at 60 °C for 30 h. The reaction mixture was cooled to room temperature and concentrated under reduced pressure to afford a colourless solid. Crystallization from a mixture of CH_2Cl_2–CH_3OH (2:1, v/v) afforded compound **2** as colourless prisms (240 mg, 76%). Mp: 157.5 °C; IR: ν_{max}(KBr) = 3294 (NH_2) and 1635 (C=O) cm^{-1}. ^{1}H NMR (300 MHz, $CDCl_3$): δ = 1.17 (6H, m, CH_3), 3.38 (4H, m, CH_2), 4.07 (1H, s, N*H*), 4.72 (2H, s, CH_2O), 6.97 (2H, d, *J* = 8.22 Hz, Ar-*H*), 7.54 (2H, s, NH_2) and 7.72 (2H, d, *J* = 8.22 Hz, Ar-*H*) ppm. ^{13}C NMR (100 MHz, $CDCl_3$): δ= 12.8 (*C*H_3), 40.4 (*C*H_2), 67.2 (*C*H_2), 114.2 (Ar-*C*), 125.7 (Ar-*C*), 128.7 (Ar-*C*), 160.9 (Ar-*C*), 166.3 (*C*=O) and 168.1 (*C*=O) ppm. FABMS: *m/z* 266.16 [M^+]. Anal. calcd. for $C_{13}H_{19}N_3O_3$: C, 58.84; H, 7.22; N, 15.84. Found: C, 59.17; H, 7.16; N, 15.76.

*4.2.2. Synthesis of Receptor **L1**.* A solution of 1-pyrenecarbaldehyde (40 mg, 0.15 mmol) in methanol (5.0 mL) was added to a solution of **2** (39 mg, 0.17 mmol) in a 1:1 mixture of chloroform and methanol (20 mL). The mixture was heated at reflux for 24 h and concentrated under reduced pressure, to afford a yellow solid. Crystallization from a mixture of chloroform–methanol (3:1, v/v) afforded compound **L1** as a light yellow solid (50 mg, 69%). Mp: 253.5 °C. IR: ν_{max}(KBr) = 1650 (CH=N and C=O), 3256 (NH) cm^{-1}. ^{1}H NMR (400 MHz, $CDCl_3$ / DMSO = 9:3): δ = 1.03 (6H, m, CH_3), 3.20 (4H, m, CH_2), 4.70 (2H, s, OCH_2), 6.93 (2H, d, *J* = 8 Hz, Ar-*H*), 7.99 (2H, d, *J* = 8 Hz, Ar-*H*), 8.61 (1H, d, *J* = 12 Hz, Py-*H*), 7.91–8.23 (8H, m, Py-*H*), 9.44 (1H, s, *H*C=N) and 11.55 (1H, s, N*H*) ppm. ^{13}C NMR (100 MHz, $CDCl_3$/DMSO = 9:3): δ = 13.6 (*C*H_3), 41.0 (*C*H_2), 67.1 (*C*H_2), 114.6–132.7 (Ar-*C*, Py-C), 146.7 (*C*=N), 161.2 (Ar-*C*), 163.9 (*C*=O) and 166.3 (*C*=O) ppm. FABMS: *m/z* 478.21 [M^+]. Anal. calcd. for $C_{30}H_{27}O_3N_3$: C, 75.45; H, 5.70; N, 8.80. Found: C, 75.26; H, 5.31; N, 8.57%.

Acknowledgments

This work was performed under the Cooperative Research Program of "Network Joint Research Center for Materials and Devices (Institute for Materials Chemistry and Engineering, Kyushu University)". We would like to thank the OTEC at Saga University and the International Collaborative Project Fund of Guizhou province at Guizhou University for financial support. CR thanks the EPSRC for a travel grant. The computational work has been assisted by the use of computing resources provided by WestGrid and Compute/Calcul Canada for which Dr. Grigory Shamov's assistance is thanked.

Supplementary data

Electronic Supplementary Information (ESI) available: Details of the NMR spectra and titration experimental data. See DOI: 10.1039/b000000x/

References and Notes

1. X. Li, X. Gao, W. Shi and H. Ma, *Chem. Rev*. **2014**, *114*, 590–659.
2. K. P. Carter, A. M. Young and A. E. Palmer, *Chem. Rev.*, **2014**, *114*, 4564–4601.
3. M. Formica, V. Fusi, L. Giorgi and M. Micheloni, *Coord. Chem. Rev.* **2012**, *256*, 170–192.
4. J. S. Lippard and M. J. Berg, *Principles of Bioinorganic Chemistry*; University Science Books: Mill Valley, CA, 1994.
5. (*a*) G. Muthup, A. Schlicksupp, L. Hess, D. Beher, T. Ruppert, C. L. Masters and K. Beyreuther, *Science.* **1996**, *271*, 1406–1409; (*b*) A. R. Løvstad, *BioMetals.* **2004**, *17*, 111–113.
6. (*a*) G. D. Barceloux, and D. D Barceloux, *J. Toxicol.-Clin. Toxicol.*, **1999**, 37, 217–230; (*b*) X. B. Zhang, J. Peng, G. L. Shen and R. Q. Yu, *Anal. Chim. Acta*. **2006**, *567*, 189-195; (*c*) L. E. Que, W. D. Domaille and C. Chang, *Chem. Rev.* **2008**, *108*, 1517–1549.
7. (*a*) Y. Zheng, K. M. Gattas-Asfura, V. Konka and R. M. Leblanc, *Chem. Commun.* **2002**, *20*, 2350–2351; (*b*) L. Zeng, E. W. Miller, A. Pralle, E. Y. Isacoff and C. J. Chang, *J. Am. Chem. Soc*. **2006**, *128*, 10–11; (*c*) X. Qi, E. J. Jun, L. Xu, S. Kim, J. S. J. Hong, Y. J. Yoon and J. Yoon, *J. Org. Chem.* **2006**, *71*, 2881–2884; (*d*) J. Liu and Y. Lu, *J. Am. Chem. Soc*. **2007**, *129*, 9838–9839; (*e*) S. Wu, R. Huang and K. Du, *Dalton Trans*. **2009**, *24*, 4735–4740; (*f*) S. Wu and S. Liu, *Sens. Actuators. B.* **2009**, *141*, 187–191.
8. (*a*) E. Kimura, S. Aoki, E. Kikuta and T. Koike, *Proc. Natl. Acad. Sci. U. S. A.* **2003**, *100*, 3731-3736; (*b*) Y. Mikata, M. Wakamatsu and S. Yano, *Dalton Trans.* **2005**, *3*, 545–550; (*c*) K. Komatsu, Y. Urano, H. Kojima and T. Nagano, *J. Am. Chem. Soc*. **2007**, *129*, 13447–13454; (*d*) X. Chen, J. Shi, Y. Li, F. Wang, X. Wu, Q. Guo and L. Liu, *Org. Lett.* **2009**, *11*, 4426–4429; (*e*) L. Xue, C. Liu and H. Jiang, *Chem. Commun.* **2009**, *9*, 1061–1063.
9. H. Irving and R. J. P. Williams, *J. Chem. Soc*. **1953**, 3192–3210.
10. (*a*) C. Y. Lai, B. G. Trewyn, D. M. Jeftinija, K. Jeftinija, S. Su, S. Jeftinija and S. Y. V. Lin, *J. Am.Chem. Soc.* **2003**, *125*, 4451–4459; (*b*) M. Numata, C. Li, A. H. Bae, K. Kaneko, K. Sakurai and S. Shinkai, *Chem. Commun.* **2005**, *37*, 4655–4657.
11. (*a*) P. A. de Silva, N. Q. H. Gunaratne, A. T. Gunnlaugsson, M. T. Huxley, P. C. McCoy, T. J. Rademacher and E. T. Rice, *Chem. Rev.* **1997**, *97*, 1515–1567; (*b*) F. J. Callan, P. A. de Silva and C. D. Magri, *Tetrahedron.* **2005**, *61*, 8551–8588; (*c*) S. J. Kim and T. D. Quang, *Chem. Rev*, **2007**, *107*, 3780–3799; (*d*) B. Liu and H. Tian, *Chem. Commun*. **2005**, *25*, 3156–3158; (*e*) X. Qi, J. E. Jun, L. Xu, J. S. Kim, J. S. J. Hong and J. Y. Yoon, *J. Org. Chem.* **2006**, *71*, 2881–2884; (*f*) H. S. Kim, J. S. Kim, M. S. Park and K. S. Chang, *Org. Lett*. **2006**, *8*, 371–374; (*g*) S. H. Jung, S. P. Kwon, W. J. Lee, I. J. Kim, S. C. Hong, W. J. Kim, S. Yan, Y. J. Lee, H. J. Lee, T. Joo and S. J. Kim, *J. Am. Chem. Soc*. **2009**, *131*, 2008–2012; (*h*) X. Huang, Z. Guo, W. Zhu, Y. Xie and H. Tian, *Chem. Commun.* **2008**, *77*, 5143–5145.
12. (*a*) V. Dujols, F. Ford and W. A. Czarnik, *J. Am. Chem. Soc*. **1997**, *119*, 7386–7387; (*b*) J. Liu and Y. Lu, *J. Am. Chem. Soc.* **2007**, *129*, 9838–9839; (*c*) K. W. K. Swamy, K. S. Ko, H. Lee, C. Mao, M. J. Kim, H. K. Lee, J. Kim, I. Shin and J. Yoon, *Chem. Commun*. **2008**, *45*, 5915–5917; (*d*) X. Chen, M. Jou, H. Lee, S. Kou, J. Lim, W. S. Nam, S. Park, M. -K. Kim and J. Yoon, *Sens and Actuators B.* **2009**, *137*, 597–602; (*e*) Z. C. Wen, R. Yang, H. He and Y. B. Jiang, *Chem. Commun*. **2006**, *42*, 106–108.
13. (*a*) V. A. Varnes, B. R. Dodson and L. E. Whery, *J. Am. Chem. Soc.* **1972**, *94*, 946–950; (*b*) A. J. Kemlo and M. T. Shepherd, *Chem. Phys. Lett.* **1977**, *47*, 158–162; (*c*) K. Rurack, U. Resch, M. Sensoer and S. Daehne, *J Fluoresc.* **1993**, *3*, 141–143.
14. K. Li, N. Li, X. Chen and A. Tong, *Anal. Chim. Acta*. **2012**, *712*, 115–119.
15. K. Rurack, U. Resch-Genger and W. Rettig, *J. Photochem. Photobiol. A. Chem.* **1998**, *118*, 143–149.
16. Y. Zhou, F, Wang, Y. Kim, J. S. Kim and J. Yoon, *Org. Lett*. **2009**, *11*, 4442–4445;
17. (*a*) K. Hanaoka, Y. Muramatsu, Y. Urano, T. Terai and T. Nagano, *Chem.–Eur. J*. **2010**, *16*, 568–572; (*b*) Y. Chen, C. Zhu, Z. Yang, J. Li, Y. Chiao, W. He, J. Chen and Z. Guo, *Chem. Commun*. **2012**, *48*, 5094–5096; (*c*) J. Wu, W. Liu, J. Ge, H. Zhang and P. Wang, *Chem. Soc. Rev.* **2011**, *40*, 3483–3495; (*d*) J. Zhao, S. Ji, Y. Chen, H. Guo and P. Yang, *Phys. Chem. Chem. Phys.* **2012**, *14*, 8803; (*e*) J. B. Birks, M. D. Lumb, I. H. Munro, *Proc. R. Soc. London* **1964**, A280, 289; (*f*) I. Takashima, M. Kinoshita, R. Kawagoe, S. Nakagawa, M. Sugimoto, I. Hamachi and A. Ojida, *Chem.−Eur. J.* **2014**, *20*, 2184−2192.
18. (*a*) M. F. Winnik, *Chem. Rev*. **1993**, *93*, 587–614; (*b*) C. Yao, B. H. Kraatz and P. R. Steer, *Photochem. Photobiol. Sci.* **2005**, *4*, 191−199; (*c*) B. J. Birks, *Rep. Prog. Phys.* **1975**, *38*, 903−974.
19. (*a*) E. Manandhar and J. K. Wallace, *Inorg. Chim. Acta*. **2012**, *381*, 15−43; (*b*) S. Karuppannan and C. J. Chambron, *Chem. Asian J*. **2011**, *6*, 964−984; (*c*) Y. Zhou, C. Zhu, S. X. Gao, Y. X. You and C. Yao, *Org. Lett.* **2010**, *12*, 2566−2569; (*d*) R. Martínez, A. Espinosa, A. Tárraga and P. Molina, *Tetrahedron.* **2010**, *66*, 3662−3667; (*e*) V. Chandrasekhar and D. M. Pandey, *Tetrahedron Lett*. **2011**, *52*, 1938−1941; (*f*) L. X. Ni, S. Wang, X. Zeng, Z. Tao and T. Yamato, *Org. Lett*. **2011**, *13*, 552−555; (*g*) H. S. Jung, M. Park, D. Y. Han, E. Kim, C. Lee, S. Ham and J. S. Kim, *Org. Lett*. **2009**, *11*, 3378−3381.
20. Y. S. Wu, C. Y. Li, Y. F. Li, D. Li and Z. Li, *Sens. Actuators B: Chem.* **2016**, *222*, 1226–1232.
21. P. Venkatesan and S. P. Wu, *RSC Adv*. **2015**, *5*, 42591–42596.

22. S. P. Wu, Z. M. Huang, S. R. Liu and P. K. Chung, *J Fluoresc.* **2012**, *22*, 253–259.
23. Nagaraju and S. Pal, *J. Organomet. Chem*. **2013**, *737*, 7–11.
24. P. S. Lee and N. Yoshikai, *Angew. Chem*. **2013**, *52*, 1240–1242.
25. (*a*) P. Thordarson., *Chem. Soc. Rev*. **2011**, *40*, 1305–1323; (*b*) **http://supramolecular.org**; (*c*) H. A. Benesi and J. H. Hildebrand, *J. Am. Chem. Soc*. **1949**, *71*, 2703–2707.
26. (*a*) S. Goswami, A. K. Das and S. Maity, *Dalton Trans.* **2013**, *42*, 16259−16263; (*b*) L. Porrès, A. Holland, L.-O. Pålsson, A. P. Monkman, C. Kemp and A. Beeby, *J Fluoresc*. **2006**, *16*, 267–272.
27. (*a*) J. P. Perdew, K. Burke and Ernzerhof, M. *Phys. Rev. Let*. **1996**, *77*, 3865–3868; (*b*) J. P. Perdew, K. Burke and Ernzerhof, M. *Phys. Rev. Let.* **1997**, *78*, 1396.
28. (*a*) P. J. Hay and W. R. Wadt, *J. Chem. Phys.* **1985**, *82*, 270; (*b*) P. J. Hay, W. R. Wadt, *J. Chem. Phys.* **1985**, *82*, 284; (*c*) P. J. Hay and W. R. Wadt, *J. Chem. Phys*. **1985**, *82*, 299.
29. Initial molecular modeling calculations using the MMFF94 method were performed using the *PC Spartan'10* software from Wavefunction Inc., Irvine CA.M.
30. M. J. Frisch, G. W. Trucks, H. B. Schlegel, G. E. Scuseria, M. A. Robb, J. R.Cheeseman, G. Scalmani, V. Barone, B. Mennucci, G. A. Petersson, H. Nakatsuji, M. Caricato, X. Li, H. P. Hratchian, A. F. Izmaylov, J. Bloino, G. Zheng, J. L. Sonnenberg, M. Hada, M. Ehara, K. Toyota, R. Fukuda, J. Hasegawa, M. Ishida, T. Nakajima, Y. Honda, O. Kitao, H. Nakai, Jr. T. Vreven, J. A. Montgomery, J. E. Peralta, F. Ogliaro, M. Bearpark, J. J. Heyd, E. Brothers, K. N. Kudin, V. N. Staroverov, T. Keith, R. Kobayashi, J. Normand, K. Raghavachari, A. Rendell, J. C. Burant, S. S. Iyengar, J. Tomasi, M. Cossi, N. Rega, J. M. Millam, M. Klene, J. E. Knox, J. B. Cross, V. Bakken, C. Adamo, J. Jaramillo, R. Gomperts, R. E. Stratmann, O. Yazyev, A. J. Austin, R. Cammi, C. Pomelli, J. W. Ochterski, R. L. Martin, K. Morokuma, V. G. Zakrzewski, G. A. Voth, P. Salvador, J. J. Dannenberg, S. Dapprich, A. D. Daniels, O. Farkas, J. B. Foresman, J. V. Ortiz, J. Cioslowski and D. J. Fox, Gaussian 09, Revision D.01; Gaussian, Inc., Wallingford CT, **2013**.